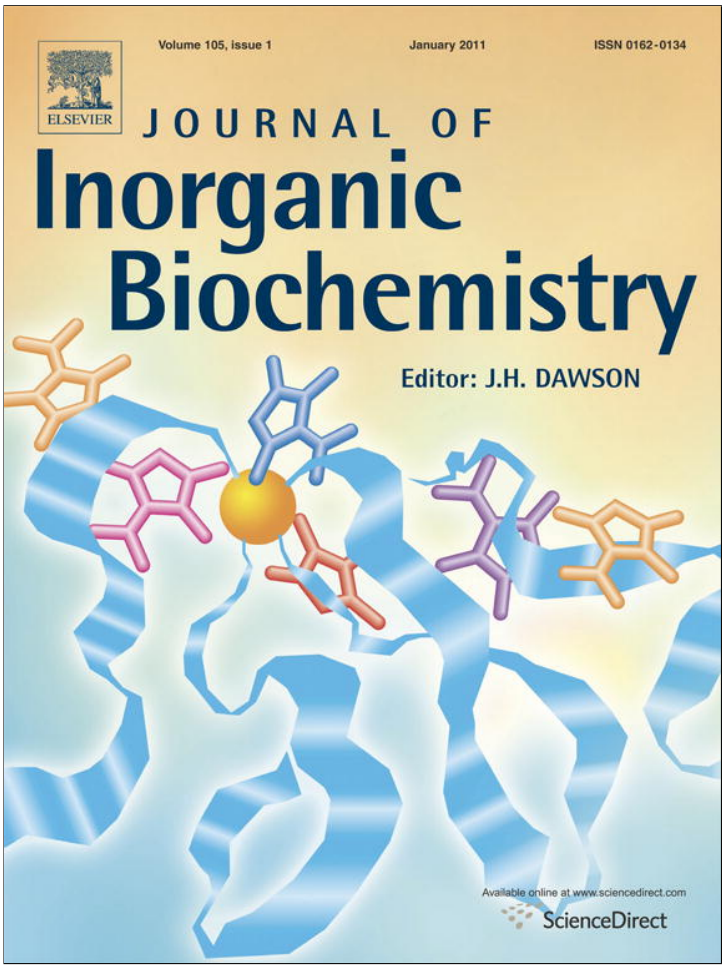

(This is a sample cover image for this issue. The actual cover is not yet available at this time.)

Journal of Inorganic Biochemistry 105 (2011) 637–644

Contents lists available at ScienceDirect

Journal of Inorganic Biochemistry

journal homepage: www.elsevier.com/locate/jinorgbio

Copper(II) complexes with tridentate pyrazole-based ligands: synthesis, characterization, DNA cleavage activity and cytotoxicity

Sofia Gama [a], Filipa Mendes [a], Fernanda Marques [a], Isabel C. Santos [a], M. Fernanda Carvalho [b], Isabel Correia [b], João Costa Pessoa [b], Isabel Santos [a], António Paulo [a,*]

[a] Unidade de Ciências Químicas e Radiofarmacêuticas, Instituto Tecnológico e Nuclear Estrada Nacional 10, 2686–953 Sacavém, Portugal
[b] Centro de Química Estrutural, Instituto Superior Técnico, UT Lisboa, Av. Rovisco Pais, 1049–001 Lisboa, Portugal

ARTICLE INFO

Article history:
Received 25 August 2010
Received in revised form 14 January 2011
Accepted 14 January 2011
Available online xxxx

Keywords:
Copper(II)
Pyrazole ligands
X-ray structures
DNA cleavage
Cytotoxicity

ABSTRACT

Tridentate pyrazole-containing ligands of the Schiff base type, SalPz — HL^1, Cl_2SalPz — HL^2 and I_2SalPz — HL^3, were used to prepare a series of new Cu(II) complexes (CuSalPz — **1**, $CuCl_2$SalPz — **2** and CuI_2SalPz — **3**). These new complexes have been studied by different analytical techniques (electrospray ionization mass spectrometry (ESI-MS), elemental analysis, FT-IR and EPR). The spectroscopic properties of **1**–**3** are consistent with the formation of Cu(II) complexes coordinated by monoanionic and tridentate (N,N,O)-chelators, behaving as monomeric species in aqueous solution, as shown by EPR studies. Crystals of **2** and **3**, obtained by slow concentration of methanolic solutions of the compounds, were also analyzed by X-ray diffraction analysis. The X-ray structural study has shown that **2** crystallized as a dinuclear compound, $[Cu_2(\mu\text{-}Cl)_2(Cl_2SalPz)_2]$, while the solid state structure determined for **3** is best described by monomeric units of $[CuCl(I_2SalPz)]$ displaying short Cu···Cl intermolecular contacts. The *in vitro* evaluation of **1**–**3** comprised the study of their DNA-cleaving ability using plasmid DNA and the assessment of their cytotoxic activity against several human cancer cell lines (PC-3 prostate, MCF-7 breast and A2780 and A2780cisR-ovary). The studies with plasmid DNA have shown that **2** and **3** induce extensive DNA cleavage in the presence of different additives. The cytotoxic activity of **2** and **3** is comparable to the one presented by cisplatin, with the exception of the A2780 cell line where cisplatin is more active. It has been found that the introduction of halogen substituents in the phenolate rings of the chelators enhanced the cytotoxicity of the respective Cu(II) complexes.

1. Introduction

Cancer is a leading cause of death worldwide. The clinical success of cisplatin, and related platinum based drugs, as anti-cancer agents constitutes the most important contribution to the use of metals in medicine. However, there are major concerns associated with these anti-cancer metallodrugs, which include problems with resistance, serious toxicity and other side effects [1]. The main cellular target for platinum drugs is genomic DNA, namely in case of cisplatin where the major antitumor activity results from intrastrand crosslinks and the formation of DNA kinks [2]. For this reason, considerable efforts are still ongoing to find more effective DNA targeting drugs. An alternative approach to obtain new antineoplastic metallodrugs, with DNA as a target, can rely on the evaluation of the so-called 'chemical nucleases', which can cleave DNA by several pathways, namely nucleobase oxidation, phosphate ester hydrolysis and deoxyribose sugar oxidation. The most efficient chemical nucleases contain transition metal ions, like the redox-active Cu, Fe, or the redox-inactive Zn in their active sites. Classic examples of this type of artificial nucleases used as antitumour drugs are bleomycin and some of its metal-coordinated derivatives along with $[Cu(phen)_2]^+$-based complexes [2].

Copper has a long history of medical use, and its prospective antitumor properties have attracted attention recently because it is thought to be less toxic than nonessential metals, such as platinum [3,4]. It is well-recognized that copper complexes have the ability to induce the hydrolysis or oxidative cleavage of DNA, being Cu(II) complexes among the most extensively studied chemical nucleases. Usually, the DNA cleavage activity of Cu(II) complexes is observed in the presence of oxidizing or reducing co-reactants. However, recent studies have shown that a square-planar Cu(II) complex chelated by a (N,N,O)-tridentate Schiff-base containing phenolic and pyridyl rings as coordinating groups has a remarkable capability to cleave DNA, in a catalytic way and without requiring the presence of a reductant co-factor [5–7]. The mechanism involved in such catalytic cleavage of DNA is not fully understood, being probably initiated by the intercalation of the highly planar Cu(II) complex. The use of different, but structurally related, ligands is expected to provide a better understanding of the factors that are crucial for the DNA cleavage activity of this type of complexes, allowing a more rational approach

* Corresponding author. Fax: +351 21 994 6185.
E-mail address: apaulo@itn.pt (A. Paulo).

0162-0134/$ – see front matter © 2011 Elsevier Inc. All rights reserved.
doi:10.1016/j.jinorgbio.2011.01.013

for the development of Cu(II) complexes with potential as anti-cancer drugs.

Recently, our group introduced (N,N,O)-tridentate pyrazole-imine-phenol ligands which are readily obtained by condensation of adequate N-(2-aminoethyl)pyrazole and salicylaldehyde derivatives, allowing a quite versatile introduction of different substituents at the pyrazolyl or phenolate rings. We have explored such ligands to synthesize homoleptic Ga(III) complexes, which have exhibited a weak to moderate cytotoxicity against human tumor cells with induction of cell death mainly by apoptotic pathways [8]. We anticipate that our tridentate pyrazolyl-containing ligands would be adequate to stabilize copper complexes with potential activity as chemical nucleases, as reported previously by other authors for Cu(II) complexes formed by related pyridine-containing (N,N,O)-tridentate Schiff-bases [6].

In this work, we describe novel copper(II) complexes with (N,N,O)-tridentate pyrazole-imine-phenol ligands and explore their potential application in cancer research. We have focused on 2-[2-(pyrazol-1-yl)ethyliminomethyl]phenol (HL^1) [8,9], a Schiff base resulting from the condensation of N-(2-aminoethyl)pyrazole and salicylaldehyde, and on its di-halogenated derivatives (HL^2–HL^3) (Fig. 1). HL^1–HL^3 were expected to act as mononegative and tridentate chelators providing, together with the metal-chloro core, the basic structural framework to the complexes. The respective Cu(II) complexes (**1**–**3**) were characterized in the solid state and in solution, and their redox activity was evaluated by cyclic voltammetry. The DNA cleavage ability of **1**–**3** was evaluated using circular plasmid DNA and their cytotoxicity assessed against selected human cancer cell lines.

2. Experimental section

2.1. General procedures

All chemicals used were p.a. grade. The solvents were dried using methods described in literature, when anhydrous conditions were necessary [10]. The chemical reactions were followed by TLC. ^1H and ^{13}C NMR spectra were recorded on a Varian Unity 300 MHz spectrometer, and chemical shifts are given in ppm, referenced with the residual solvent resonances relative to $SiMe_4$. IR spectra were recorded as KBr pellets on a Bruker Tensor 27 spectrometer. C, H and N analyses were performed on an EA 110 CE Instruments automatic analyzer. The EPR spectra were recorded either at room temperature or at 77 K (on glasses prepared by freezing solutions in liquid nitrogen) with a Bruker ESP 300E X-band spectrometer operating at 100 KHz.

2.2. Synthesis of the ligands

The pyrazole-imine-phenolate ligands N-(2-hydroxybenzyl-2-pyrazolethyl)imine (HL^1) and N-(2-hydroxy-3,5-dichloride-benzyl-2-pyrazolethyl)imine (HL^2) were synthesized and purified as previously described [8,9]. The new ligand, N-(2-hydroxy-3,5-diiodine-benzyl-2-pyrazolethyl)imine (HL^3), was synthesized following a similar procedure, as described below.

2.2.1. N-(2-hydroxy-3,5-diiodine-benzyl-2-pyrazolethyl)imine (HL^3)

To a solution of N-(2-aminoethyl)pyrazole (0.700 g, 6.3 mmol) in dry ethanol (30 mL) was added 2-hydroxy-3,5-diiodobenzaldehyde-salicylaldehyde (2.354 g, 6.3 mmol) and the mixture was refluxed for 2 h. After cooling to room temperature, the solvent was removed under vacuum to afford a yellow solid. Yield: 2.055 g (4.4 mmol, 70%). ^1H NMR δH (300 MHz, $CDCl_3$): 13.87 (1 H, s (singlet), OH), 8.01 (1 H, s, N = CH), 7.75 (1 H, d (doublet), H(3/5)-pz), 7.52 (1 H, d, H(3/5),pz), 7.34 (1 H, m (multiplet), Ph), 7.28 (1 H, m, Ph), 6.16 (1 H, tr (triplet), H (4)-pz), 4.44 (2 H, tr, N-CH_2), 4.06 (2 H, pz-CH_2). IR (KBr, cm^{-1}): 1661 ($\upsilon_{C=N}$). m/z (ESI-MS): 465.9 $[L^3\text{-H}]^-$ (calc. 465.89), 467.8 $[L^3 + H]^+$ (calc. 467.91), 489.7 $[L^3 + Na]^+$ (calc. 489.89). Element. Anal. (%). Found: C 30.36, H 2.75, N 8.95. Calc. for $C_{12}H_{11}I_2N_3O{\cdot}0.5H_2O$: C 30.28, H 2.54, N 8.83.

2.3. Synthesis of the copper(II) complexes

2.3.1. Chloro [N-(2-hydroxybenzyl-2-pyrazolethyl)iminate] copper(II) (1)

To a solution of N-(2-hydroxybenzyl-2-pyrazolethyl)imine (HL^1) (200 mg, 0.93 mmol) in methanol (5 mL) was slowly added $CuCl_2$. H_2O (158 mg, 0.93 mmol) previously dissolved in methanol (2 mL). The mixture was stirred at room temperature for 2 h. The formed dark green precipitate was recovered by centrifugation, washed with cold methanol and dried under vacuum. Yield: 154 mg (0.49 mmol, 53%). IR (KBr, cm^{-1}): 1622 ($\upsilon_{C=N}$). m/z (ESI-MS): 276.9 $[CuL^1]^+$ (calc. 277.03). Element. Anal. (%). Found: C 41.97, H 3.86, N 12.12. Calc. for $C_{12}H_{12}ClCuN_3O{\cdot}1.5H_2O$: C 42.36, H 4.44, N 12.35.

2.3.2. Chloro [N-(2-hydroxy-3,5-dichloride-benzyl-2-pyrazolethyl) iminate] copper(II) (2)

Complex **2** was obtained by reacting $CuCl_2$ with HL^2, as above described for **1**. **2** was recovered as a green microcrystalline solid. Yield: 168 mg (0.44 mmol, 63%). IR (KBr, cm^{-1}): 1628 ($\upsilon_{C=N}$). m/z (ESI-MS): 346.8 $[CuL^2]^+$ (calc. 346.95). Element. Anal. (%). Found: C 36.63, H 2.08, N 10.85. Calc. for $C_{12}H_{10}Cl_3CuN_3O.0.5H_2O$: C 36.85, H 2.83, N 10.74.

2.3.3. Chloro [N-(2-hydroxy-3,5- diiodine-benzyl-2-pyrazolethyl) iminate] copper(II) (3)

Starting from $CuCl_2$ and HL^3, **3** was synthesized and purified using the same procedure above described for **1** and **2**, being obtained as a green microcrystalline solid. Yield: 153 mg (0.27 mmol, 61%). IR (KBr, cm^{-1}): 1627 ($\upsilon_{C=N}$). m/z (ESI-MS): 528.7 $[CuL^3]^+$ (calc. 528.82). Element. Anal. (%). Found: C 25.81, H 2.14, N 7.90. Calc. for $C_{12}H_{10}ClCuI_2N_3O$: C 25.51, H 1.78, N 7.44.

2.4. X-ray diffraction analysis

Green crystals of **2** and **3** suitable for X-ray diffraction studies were obtained from a methanolic solution of the complexes, after standing for three weeks. The X-ray diffraction analysis of **2** and **3** was performed on a Bruker AXS APEX CCD area detector diffractometer, using graphite monochromated Mo Kα radiation (0.71073 Å). Empirical absorption correction was carried out using SADABS program [11]. Data collection and data reduction were done with the SMART and SAINT programs [12]. The structures were solved by direct methods with SIR97 [13] and refined by full-matrix least-squares analysis with SHELXL-97 [14] using the WINGX [15] suite of programs. All non-hydrogen atoms were refined anisotropically. The remaining hydrogen atoms were placed in calculated positions. Molecular graphics were prepared using ORTEP3 [16]. A summary of the crystal data, structure solution and refinement parameters are given in Table 1.

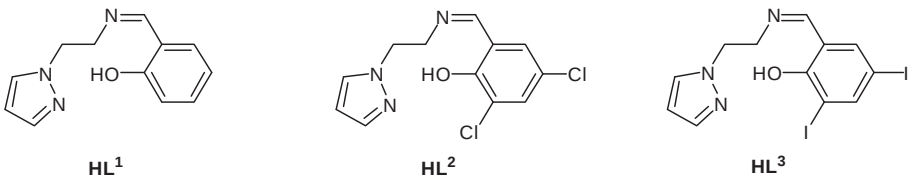

Fig. 1. Tridentate pyrazole-containing ligands of the Schiff base type (L^1–L^3) used to prepare the Cu(II) complexes.

Table 1
Crystallographic data for **2** and **3**.

	2	**3**
Formula	$C_{24}H_{20}Cl_6Cu_2N_6O_2$	$C_{24}H_{20}Cl_2Cu_2I_4N_6O_2$
Formula weight	764.24	1130.04
T/K	150(2)	150(2)
Crystal system	Triclinic	Monoclinic
Space group	P_{-1}	P12(1)/c1
a/Å	7.0735(2)	12.1865(4)
b/Å	12.3713(3)	9.2419(3)
c/Å	15.7347(4)	27.6805(10)
α/°	83.529(1)	90
β/°	85.994(1)	93.323(1)
γ/°	81.393(1)	90
V/Å^3	1350.77(6)	3122.31(18)
Z	2	4
D_x/g cm^{-3}	1.879	2.412
μ/mm^{-1}	2.206	5.540
F(000)	764	2104
Crystal size/mm	0.20×0.10×0.04	0.20×0.10×0.04
R(int)	0.0470	0.0435
Number of reflections collected	11,151	21,117
Number of unique reflections	5499	5900
Goodness-of-fit on F^2	1.016	1.165
R_1[a]	0.0508	0.0483
wR_2 (all data) [a]	0.0893	0.0773

[a] $R_1 = \Sigma||F_0| - |F_c||/\Sigma|F_0|$, $wR_2 = \{\Sigma[w(||F_0|^2 - |F_c|^2|)^2]/\Sigma[w(F_0^4)]\}^{1/2}$.

2.5. Electrochemical properties

The cyclic voltammetry studies were performed under dinitrogen in a potentiostat/galvanostat Radiometer Analytical Voltammetry PST050 VoltaLab® equipment, using a Pt wire as working electrode and MeOH or tetrahydrofuran (THF) solutions of $[NBu_4][BF_4]$/(0.1 M) as electrolyte. The solvents (THF, Merck and MeOH Sigma-Aldrich) were purified by conventional techniques and distilled immediately before use. The potentials were measured at 200 mV/s using $[Fe(\eta^5\text{–}C_5H_5)_2]^{0/+}$ ($E_{½}$ = 0.547 V *vs.* saturated calomel electrode (SCE)) as internal reference [17].

2.6. DNA cleavage activity

The plasmid DNA used for gel electrophoresis experiments was PhiX174 (Promega). Linear DNA was obtained by digestion with the single-cutter restriction enzyme *XhoI* and used as a reference in agarose gel electrophoresis. DNA cleavage activity was evaluated by monitoring the conversion of supercoiled plasmid DNA (Sc — form I) to nicked circular DNA (Nck — form II) and linear DNA (Lin — form III).

Each reaction mixture was prepared by adding 6 μL of water, 2 μL (200 ng) of supercoiled DNA, 2 μL of 100 mM stock Na_2HPO_4/HCl pH 7.2 buffer solution and 10 μL of the aqueous solution of the complex. The final reaction volume was 20 μL, the final buffer concentration was 10 mM and the final metal concentration varied from 50 to 250 μM. Samples were typically incubated for 18 h at 37 °C. When indicated, the reaction was carried out in the same buffer but in the presence of ascorbic acid (10 μM), H_2O_2 (50 μM), DMSO (5%) or in the dark.

After incubation, 5 μL of DNA loading buffer (0.25% bromophenol blue, 0.25% xylene cyanol, 30% glycerol in water, Applichem) were added to each tube and the sample was loaded onto a 0.8% agarose gel in TBE buffer (89 mM Tris–borate, 1 mM EDTA pH 8.3) containing ethidium bromide (0.5 μg/mL). Controls of non-incubated and of linearized plasmid were loaded on each gel electrophoresis. The electrophoresis was carried out for 2.5 h at 100 V. Bands were visualized under UV light and images captured using an AlphaImagerEP (Alpha Innotech). Peak areas were measured by densitometry using AlphaView Software (Alpha Innotech). Peak areas were used to calculate the percentage (%) of each form (Sc, Nck and Lin), with a correction factor of 1.47 for the Sc form to account for its lower staining capacity by ethidium bromide [18].

The photos chosen for this publication were rearranged to show only the relevant samples. All samples in each figure were obtained from the same run.

2.7. Cell viability assays in human tumor cell lines

The tumor cell lines MCF-7, PC-3, A2780 and A2780cisR (ATCC), were cultured in DMEM (Dulbecco's Modified Eagle Medium) containing GlutaMax I (MCF-7) and RPMI 1640 (PC-3, A2780 and A2780cisR) culture medium (Invitrogen) supplemented with 10% FBS and 1% penicillin/streptomycin at 37 °C in a humidified atmosphere of 95% of air and 5% CO_2 (Heraeus, Germany). Cell viability was evaluated using a colorimetric method based on the tetrazolium salt MTT ([3-(4,5-dimethylthiazol-2-yl)-2,5-diphenyltetrazolium bromide]), which is reduced in viable cells to yield purple formazan crystals. Cells were seeded in 96-well plates at a density of 2×10^4 cells (PC-3) and 5×10^4 cells (MCF-7) per well in 200 μL of culture medium and left to incubate overnight for optimal adherence. After careful removal of the medium, 200 μL of a dilution series of the compounds in fresh medium were added and incubation was performed at 37 °C/5% CO_2 for 24 h. The percentage of DMSO in cell culture medium did not exceed 1%. Cisplatin was first solubilized in saline and then added at the same concentrations used for the other compounds. At the end of the incubation period, the compounds were removed and the cells were incubated with 200 μL of MTT solution (500 μg/mL). After 3–4 h at 37 °C/5% CO_2, the medium was removed and the purple formazan crystals were dissolved in 200 μL of DMSO by shaking. The cell viability was evaluated by measurement of the absorbance at 570 nm using a plate spectrophotometer (Power Wave Xs, Bio-Tek). The cell viability was calculated dividing the absorbance of each well by that of the control wells (cells treated with medium containing 1% DMSO). Each experiment was repeated at least three times and each point was determined in at least six replicates.

Statistical analysis (F-test) was done with GraphPad Prism software to assess if there was a significant difference between the IC50 values of complexes **1**–**3** and corresponding ligands HL^1–HL^3.

3. Results and discussion

3.1. Synthesis and characterization

The syntheses of the Cu(II) complexes with the tridentate pyrazole-containing ligands of the Schiff base type (HL^1–HL^3) were done using a common procedure, by reaction of a stoichiometric amount of $CuCl_2.H_2O$ with the corresponding ligand, in methanol. The resulting complexes, **1**–**3**, precipitated as green microcrystalline solids that were analyzed by ESI-MS, elemental analysis, FT-IR and EPR. Their characterization in solution was also done by EPR spectroscopy and by cyclic voltammetry. **2** and **3** were also studied by X-ray diffraction analysis. As discussed below the analytical data obtained for **1**–**3** are consistent with the formation of chloro complexes of Cu(II) coordinated by (N, N, O)-tridentate chelators, as confirmed by X-ray diffraction analysis in the case of **2** and **3**.

The most relevant feature of the IR spectra of **1**–**3** is the red shift of the ν(C=N) bands upon coordination of HL^1–HL^3 to the metal ion, ranging from $\Delta\nu$ = 19 cm^{-1} (**1**) to $\Delta\nu$ = 70 cm^{-1} (**2**). The positive-ion ESI mass spectra of the complexes in MeOH showed in all cases an intense peak corresponding to the loss of the chloride co-ligand (m/z = $[CuL^x]^+$) with the expected isotopic patterns. These data are consistent with the coordination of tridentate and monoanionic chelators (L^1–L^3) to Cu(II) metal ions.

Although the analysis data for "H" are somewhat unsatisfactory, in particular for compound **2**, the IR and ESI-MS analysis results and, most definitively, the X-ray crystallographic data support the formula.

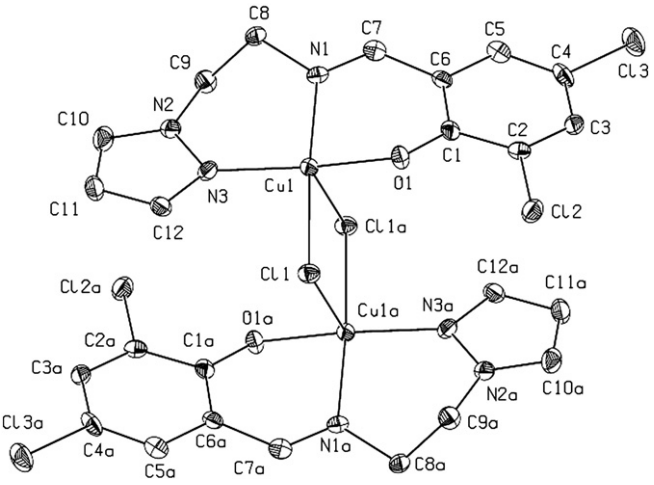

Fig. 2. ORTEP view of **2**. Ellipsoids are draw at the 40% probability level.

3.2. X-ray crystal structures

In the solid state, compound **2** presents a dinuclear structure with the two copper(II) atoms linked through two μ-Cl bridges. The structure of **3** consists of monomeric units of [CuCl(I_2SalPz)] displaying short Cu···Cl intermolecular contacts. Two crystallographic and chemically independent [CuCl(I_2SalPz)] units are present in the asymmetric unit of **3**. An ORTEP view of the dimeric structure of **2**, together with the respective atom-labeling scheme, is depicted in Fig. 2. Fig. 3 shows an ORTEP diagram of one of the independent molecules of **3** (Fig. 3a), as well as a view of the packing diagram of **3** (Fig. 3b). Selected bond distances and angles of the solid state structures of **2** and **3** are presented in Table 2.

Each copper atom of the dinuclear unit of **2** is five-coordinated in a distorted square pyramidal environment, with the basal positions being occupied by the tricoordinated pyrazolyl-containing ligand and by one of the bridging chloride atoms. Analysis of the shape determining angles, α and β (the two largest angles around the central atom) [19] yields a value for the trigonality index, τ [$\tau = (\alpha-\beta)/60$], of 0.16. According to it ($\tau = 0$ and 1 for perfect square pyramidal and trigonal bipyramidal geometries, respectively), the geometry around copper can be described as a distorted square pyramid.

The bridging Cu_2Cl_2 unit is constrained to be planar by the presence of a crystallographic inversion center in the middle of this unit. Each bridging chloride simultaneously occupies a basal position of the coordination polyhedron of one Cu(II) ion and an apical site of the other Cu(II) ion. For the tridentate and monoanionic ligand, the Cu(1)–$O_{phenolate}$ (1.889(2) Å), the Cu(1)–N_{imine} (1.998(2) Å) and Cu(1)–$N_{pyrazolyl}$ (1.998(2) Å) bond distances are comparable with those reported for other Cu(II) complexes with related tridentate ligands of the Schiff base type [20]. The Cu–Cl distances are different from one another, being the apical Cu–Cl(1) distance considerably longer than the equatorial one [2.2989(8) *vs.* 2.7598(8) Å] as reported for other dichloro-bridged Cu(II) complexes [20–22]. The Cu(1)–Cu(1a) separation of *ca.* 3.6 Å and the bridging angle Cu(1)–Cl(1)–Cu(1a) of 90.47(3)° are well within the range of values (3.42–4.09 Å and 84.9–96.8°, respectively) found for other dimeric copper complexes containing the bridging Cu_2Cl_2 unit [20,21,23–32].

Each of the two independent molecules of **3** display a square planar coordination geometry around the Cu atoms (Fig. 3), which is defined by the coordinated oxygen and nitrogen atoms from the tridentate anchor ligand and by the chloride co-ligand. For both independent molecules, the distances Cu–$O_{phenolate}$, Cu–N_{imine}, Cu–$N_{pyrazolyl}$ and Cu–Cl are very similar and can be considered comparable to those found for **2**. The packing of the molecules of **3** involves short Cu Cl intermolecular contacts (2.9220(1) Å) between the copper atom (Cu(2)) of molecule 2 and the equatorial chloride coordinated to the copper atom (Cu(I)) of molecule 1. This distance is considerably longer than the calculated average value [2.554(100) Å] for eleven copper(II) complexes with Cu–Cl bridging bond distances considered long (>2.50 Å), and we therefore conclude it is a short intermolecular contact [33]. As shown in Fig. 3, there is an almost coplanarity between the independent molecules of each type, which

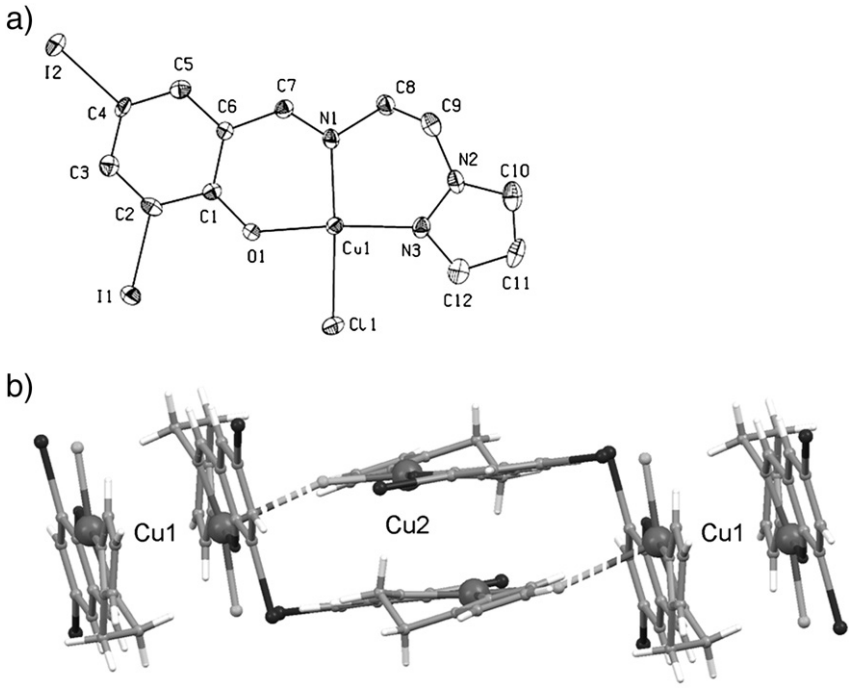

Fig. 3. ORTEP view of **3** (a) with a view of its packing diagram (b). Ellipsoids are draw at the 40% probability level.

Table 2
Selected bond lengths (Å) and angles (°) for complexes **2** and **3**.

Bond lengths (Å)		Bond angles (°)		Bond lengths (Å)		Bond angles (°)	
Cu(1)–O(1)	1.899(2)	O(1)–Cu(1)–N(3)	165.69(10)	Cu(1)–O(1)	1.906(4)	O(1)–Cu(1)–N(3)	173.8(2)
Cu(1)–N(3)	1.990(3)	O(1)–Cu(1)–N(1)	89.17(10)	Cu(1)–N(3)	1.989(5)	O(1)–Cu(1)–N(1)	91.9(2)
Cu(1)–N(1)	1.998(2)	N(3)–Cu(1)–N(1)	93.53(10)	Cu(1)–N(1)	1.993(5)	N(2)–Cu(1)–N(1)	93.6(2)
Cu(1)–Cl(1)	2.2989(8)	O(1)–Cu(1)–Cl(1)	86.61(7)	Cu(1)–Cl(1)	2.2902(18)	O(1)–Cu(1)–Cl(1)	84.82(14)
Cu(1)–Cl(1a)	2.7598(8)	N(3)–Cu(1)–Cl(1)	90.96(8)	Cu(2)–O(2)	1.903(4)	N(3)–Cu(1)–Cl(1)	89.95(17)
Cu(1a)–O(1a)	1.899(2)	N(1)–Cu(1)–Cl(1)	175.47(8)	Cu(2)–N(6)	2.020(6)	N(1)–Cu(1)–Cl(1)	174.62(17)
Cu(1a)–N(3a)	1.990(3)	O(1)–Cu(1)–Cl(1a)	95.98(7)	Cu(2)–N(4)	1.984(5)	O(2)–Cu(2)–N(6)	176.6(2)
Cu(1a)–N(1a)	1.998(2)	N(3)–Cu(1)–Cl(1a)	98.14(7)	Cu(2)–Cl(2)	2.2897(17)	O(2)–Cu(2)–N(4)	91.0(2)
Cu(1a)–Cl(1a)	2.2989(8)	N(1)–Cu(1)–Cl(1a)	88.33(7)	Cu(2)–Cl(1)	2.9220(1)	N(4)–Cu(2)–N(6)	92.4(2)
Cu(1a)–Cl(1)	2.7598(8)	Cl(1)–Cu(1)–Cl(1a)	90.47(3)	N(1)–C(7)	1.276(8)	O(2)–Cu(2)–Cl(2)	86.02(14)
N(1)–C(7)	1.277(4)	O(2)–Cu(2)–N(6)	165.36(10)	O(1)–C(1)	1.295(8)	N(6)–Cu(2)–Cl(2)	90.62(17)
O(1)–C(1)	1.289(4)	Cu(1)–Cl(1)–Cu(1a)	89.53(3)	N(2)–N(3)	1.342(8)	N(4)–Cu(2)–Cl(2)	167.74(16)
N(2)–N(3)	1.365(3)						

Table 3
Spin Hamiltonian parameters for the Cu(II) complexes obtained by computer simulation of the experimental spectra [36].

Complex	Solvent	EPR parameters				
		$g_\perp$		$g_{//}$	$A_\perp$ ($\times 10^4$ cm^{-1})	$A_{//}$ ($\times 10^4$ cm^{-1})
1	Solid	g_1	g_2	g_3		
		2.085	2.091	2.174		
	PBS	2.053		2.261	13	182
2	Solid	g_1	g_2	g_3		
		2.040	2.114	2.199		
	PBS	2.054		2.267	14	180
3	Solid	g_1	g_2	g_3		
		2.045	2.118	2.167		
	MeOH	2.056		2.266	12	181

reflects most probably the π-stack packing of the molecules in the crystals.

3.3. EPR spectroscopy

The EPR spectra of Cu(II) complexes is a useful tool for both structural and mechanistic studies, due to the d^9 configuration of Cu^{2+}. In most cases, copper(II) centers have tetrahedral, or axially elongated octahedral geometry and their EPR spectra show axial symmetry with a more intense absorption at higher field ($g_\perp$) and a less intense one at lower field ($g_{//}$). [34,35] Among other factors, the $g_{//}$ and $A_{//}$ values depend on the nature of the donor atoms, and therefore these can be used to confirm the binding mode around the metal ion. Spectroscopic studies by EPR were carried out for **1**–**3** in the solid state at 298 K. The EPR spectra of the complexes were also recorded in phosphate buffer (pH 7.4) at 77 K, in order to assess the coordination environment around copper, an important issue taking into consideration the *in vitro* biological evaluation that has been performed for **1** and **2**. In case of **3**, as it was unsoluble in phosphate buffer, the complex was dissolved in MeOH. The spin Hamiltonian parameters were obtained by computer simulation of the experimental spectra using a program from Rockenbauer and Korecz [36]. The parameters obtained by simulation are included in Table 3. The presence of clusters was detected in solution, which was probably due to aggregation of the molecules during the freezing process. Thus, the simulation of the spectra in H_2O has been done including this minor species, which improved the fitting (data not included in Table 3).

Solid-state samples are magnetically non-diluted and, therefore, it is not possible to detect hyperfine couplings or zero-field splitting interactions in the respective EPR spectra. In the solid state, the EPR spectrum of **1** at 298 K shows a slightly asymmetric singlet, while those of **2** and **3** present rhombic distortions that are stronger for **2** (Fig. 4a–c). In phosphate buffer, the spectrum of **1** shows the presence of monomers with axial symmetry and also a dimeric species (Fig. 4d). **2** presents only mononuclear species (Fig. 4e) (a slight precipitation occurred) and **3** is insoluble in this media. Thus, and in order to characterize **3** in solution, its

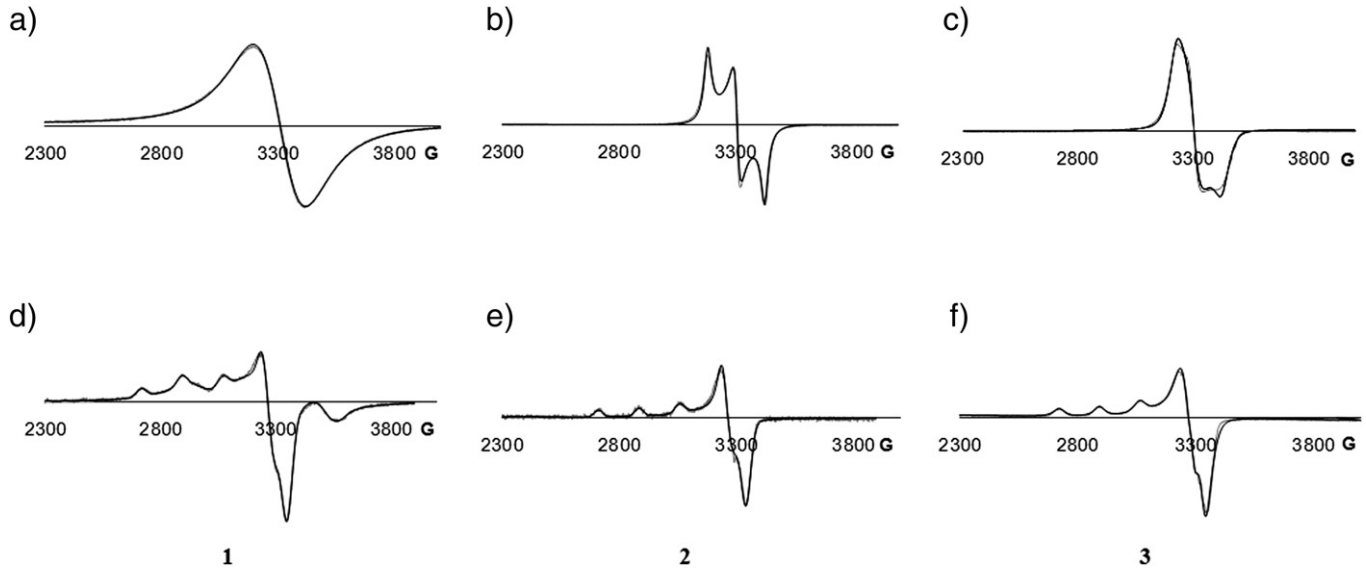

Fig. 4. EPR X-band spectra of complexes **1**(a), **2**(b) and **3**(c) in the solid state (T = 298 K); complex **1**(d) and **2**(e) in phosphate buffer (T = 77 K) and complex **3**(f) in MeOH (T = 77 K). The experimental spectra are presented at light gray and the calculated in black.

Table 4
Cyclic voltammetry data[a] for the Cu(II) complexes (**1**–**3**) and corresponding ligands (L^1–L^3).

Compound	MeOH		THF	
	E_p^{red}	E_p^{ox}	E_p^{red}	E_p^{ox}
HL^1	–	1.42	–	1.34
1	–	1.49	−1.23[b]	–
HL^2	–	1.42	–	1.62
2	−0.50	1.42	−0.51	1.50
HL^3	–	1.34	–	1.45
3	−0.52	1.45	−0.43	1.20

[a] Values in Volt (±10 mV) measured at $\nu = 200$ mV using $[Fe(\eta^5\text{–}C_5H_5)_2]^{0/+}$ (0.547 V *vs.* SCE) as internal reference.
[b] Another low intensity wave is observed ($E_p^{red} = -1.68$ V).

spectrum was measured in MeOH (Fig. 4f) and only a monomeric species was found. For all complexes, we have found that $g_{//} > g_{\perp}$ (see Table 3) either in the solid state or in solution. This point out that we are in the presence of square-planar or square-pyramidal Cu(II) complexes with the unpaired electron located at the $d_{x^2-y^2}$ orbital [37–39].

3.4. Electrochemical properties

The electrochemical behavior of Cu(II) complexes (**1**–**3**) was studied by cyclic voltammetry in MeOH and THF using $[NBu_4][BF_4]$ as electrolyte.

Complexes **2** and **3** display by cyclic voltammetry one cathodic and one anodic irreversible waves in contrast with complex **1** that displays no cathodic (MeOH) or anodic (THF) waves within the experimental potentials available for each solvent (Table 4). This behavior indicates that reduction of **1** in MeOH occurs at a considerably lower potential than reduction of **2** and **3**. This observation is confirmed by the potential of the reduction of **1** in THF (Table 4).

The cathodic waves are assigned to Cu(II) → Cu(I) reduction while the anodic waves are attributed to oxidation processes that occur at the ligands. This statement was corroborated by the study of the electrochemical behavior of the ligands in THF and MeOH. The potentials measured for the anodic waves in the ligands are well in the range of those measured for the complexes (Table 4) pointing to a ligand based process.

The mild potentials at which the cathodic processes occur in **2** and **3** may be relevant to render their reduction accessible by biological means in contrast with **1** that requires stronger reduction agents.

3.5. DNA cleavage evaluation

The effect of the various ligands (HL^1–HL^3) and respective copper complexes (**1**–**3**) on supercoiled DNA was studied using two different concentrations of the compounds at 37 °C during an 18 h incubation period in phosphate buffer (pH 7.2). After this time of incubation, all the Cu(II) complexes were able to induce conformational changes in DNA, following the same pattern but differing in the extent of the effect (Fig. 5). The interaction of these complexes with DNA gives rise to DNA isoforms, assignable to the nicked form (Form II), having lower mobility than the supercoiled form, as a result of the occurrence of single-strand breaks that were detected for a metal concentration of 50 μM. As shown in Fig. 5, an increase in concentration (to 250 μM) of the compounds led to a more pronounced DNA nicking. The supercoiled/circular ratio found for control DNA (without addition of any compound) is similar to those obtained for ligands HL^1–HL^3. In the case of **1**–**3**, this ratio decreases to values around one-half of the control. However, no effect was observed after 2 or 4 h of incubation at 37 °C even for **1**–**3** (data not shown), which indicates that these Cu(II) complexes have a low DNA-cleavage activity in the absence of any activating agent.

Since at cellular level there are agents that may be able to activate the cooper complexes to produce strand scission, further experiments were made to evaluate the effect of some activating agents as ascorbic acid (reducing agent) and/or H_2O_2 (Fig. 6).

In the presence of ascorbic acid, the three complexes show a higher nuclease activity. With **1** at 50 μM most of the supercoiled DNA is converted to nicked form and a small percentage to linear form. At higher concentrations, the nuclease activity increased with supercoiled DNA converted to the linear form and the appearance of a

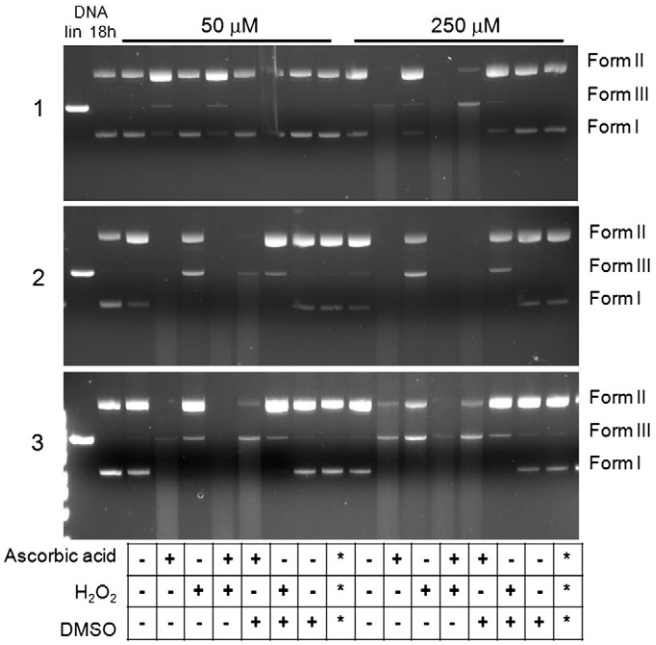

Fig. 6. Cleavage of supercoiled ϕX174 DNA by the Cu(II) complexes (**1**–**3**) after 18 h of incubation at 37 °C in phosphate buffer (pH 7.2), in the presence of reducing or oxidizing agents or in the dark (*). DNA lin — Linear DNA obtained by digestion with *XhoI*. Forms I, II and III are supercoiled, nicked circular and linear forms of DNA, respectively.

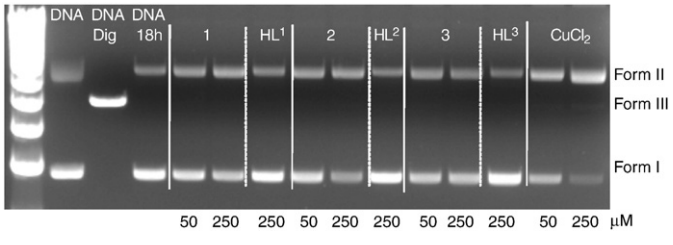

Fig. 5. Cleavage of supercoiled ϕX174 DNA by the Cu(II) complexes (**1**–**3**) and their ligands (L^1–L^3), after 18 h of incubation at 37 °C in phosphate buffer (pH 7.2). DNA Dig — Linear DNA obtained by digestion with *XhoI*. Cu — $CuCl_2$. Forms I, II and III are supercoiled, nicked circular and linear forms of DNA, respectively.

smear, indicative of extensive DNA cleavage. For **2** and **3**, this effect is much more intense, leading to the detection of the DNA smear even with the lower concentration of 50 μM. The presence of H_2O_2 has a significant effect, more remarkable for **2** and **3** where the linear form is observed in large extent.

In order to gain some insight into the possible oxidative cleavage mechanism, the effect of a hydroxyl radical scavenger (DMSO) was also tested, and no changes in the nuclease activity were observed compared with the complexes alone. This may indicate that the nuclease effect does involve the formation of oxygen based radicals. The photochemical cleavage pathway was also tested and some experiments were performed in the absence of light. Under these conditions, no effect is observed when compared with the complexes without additives.

Control experiments using only ascorbic acid, H_2O_2 and DMSO were also performed (data not shown). In the presence of ascorbic acid some single-strand breaks are detected, with the increase of the nicked circular form. However, this effect is must less intense than the one observed in the simultaneous presence of the Cu(II) complexes. The presence of only H_2O_2 and DMSO did not cause any apparent cleavage of DNA.

Therefore, we conclude that all the complexes show nuclease activity in the presence of activating agents. Complexes **2** and **3** are more efficient in the cleavage of DNA than **1**, probably due to the enhanced stabilization of the Cu(I) species, as evidenced by the highest Cu(II)/Cu(I) redox potential (Table 4).

3.6. Cytotoxic studies in cancer cell lines

The cytotoxic properties of the ligands (HL^1–HL^3) and corresponding Cu(II) complexes (**1**–**3**) were evaluated on the following human cancer cell lines: prostate cancer PC-3 cells, breast cancer MCF-7 cells, A2780 human ovarian carcinoma cells and the respective cisplatin resistant cell line (A2780cisR). For comparative purposes, such study was also performed for cisplatin and $CuCl_2$. Initially, the screening of the cytotoxic activity of the compounds has been done against the PC-3 and MCF-7 cell lines after 24 h of incubation. Then, the more active compounds were also evaluated in the A2780 and A2780cisR cell lines, using an incubation time of 72 h. The IC_{50} values were measured using a colorimetric MTT assay and are presented in Table 5.

After 24 h of incubation, the measured IC_{50} values in the PC-3 prostate and MCF-7 human breast cancer cell lines are in the 78–888 μM range, pointing out that we were in the presence of compounds having a rather low cytotoxic activity. These assays have also shown that the introduction of halogens (chloride or iodide) in the phenolic ring of the ligands enhances the cytotoxicity of the compounds. A similar effect was reported by other authors for related (N,N,O)-tridentate ligands, containing phenolic and pyridyl rings, which were used to prepare Ga (III) and Cu(II) complexes acting as proteasome inhibitors [40–42].

Both for the ligands and respective Cu(II) complexes, considerably lower IC_{50} values were obtained in the PC3 and MCF-7 cancer cell lines after 72 h of incubation. In these cell lines, the IC_{50} values ranged from 26 to 45 μM and can be considered comparable to those exhibited by cisplatin. However, there is not a considerable deference between the cytotoxicity of the ligands and corresponding complexes, except for **HL^3**/**3** where a statistically relevant ($p<0.0001$) enhancement of cytotoxic was observed on A2780 cell line. Furthermore, there is not a general improvement of the cytotoxicity by the use of the copper complexes in comparison with the stoichiometric mixture of each ligand and Cu^{2+} metal ion (data not shown).

Unlike cisplatin, HL^1–HL^3 and **1**–**3** have shown a similar cytotoxicity activity against A2780 and A2780cisR cell lines, with resistance factors (RF) factors spanning between 0.89 and 1.40 and much lower than the RF of 8.9 presented by cisplatin. This result may indicate that HL^1–HL^3 and **1**–**3** overcame cisplatin-resistance in the ovarian cancer cell lines, reflecting most probably the involvement of different mechanisms and/or targets in the cell killing.

Table 5
IC_{50} values (μM) of the Cu(II) complexes (**1**–**3**) and their ligands (HL^1–HL^3) against several human cancer cell lines ($^*p<0.05$).

Samples	24 h		72 h			
	PC-3	MCF-7	PC-3	MCF-7	A2780	A2780cisR
HL^1	522 ± 71	715 ± 167	–	–	–	–
1	365 ± 51	254 ± 47	–	–	–	–
HL^2	183 ± 28	888 ± 257	39 ± 5	32 ± 7	27 ± 5	26 ± 8
2	196 ± 18	97 ± 22	45 ± 8	31 ± 9	20 ± 6	28 ± 8
HL^3	141 ± 30	166 ± 30	32 ± 6	34 ± 7	20 ± 5*	25 ± 9
3	95 ± 40	78 ± 23	39 ± 8	26 ± 9	13 ± 4*	18 ± 4
$CuCl_2$	–	–	70 ± 20	65 ± 20	52 ± 12	–
Cisplatin	1419 ± 728	59 ± 12	51 ± 7	28 ± 6	1.9 ± 0.1	17 ± 3

4. Conclusions

New Cu(II) complexes (**1**–**3**) of pyrazolyl-containing (N,N,O)-chelators (HL^1–HL^3) were successfully synthesized, and characterized in the solid state and in solution. Its characterization in aqueous solution was done, among other techniques, by EPR, which showed the presence of monomeric species with the metal ion coordinated to the monoanionic tridentate (N,N,O)-chelators. X-ray structural analysis of crystals of **2** and **3** revealed that **2** crystallized as a dinuclear compound, while the solid state structure found for **3** is best described by monomeric units displaying short Cu···Cl intermolecular contacts.

The synthesized Cu(II) complexes exhibited a low DNA-cleavage activity in the absence of additives, inducing uniquely single-strand cleavage on plasmid DNA, together with moderate cytotoxicity against different human tumor cell lines. However, all the complexes have shown an enhanced nuclease activity in the presence of additives, namely in the presence of ascorbic acid. The measured cytotoxicity and DNA cleavage ability follows the order **3** (iodo)>**2** (chloro)>**1** (H). Such trend may reflect the enhanced stabilization of Cu(I) species in the case of **2** and **3**, due to their highest Cu(II)/Cu(I) redox potential as a result of the π-donating effect of the halogen substituent group at the phenolate ring.

Acknowledgments

The authors thank the financial support from the Portuguese Fundação para a Ciência e Tecnologia through the grant SFRH/BPD/29564/2006. J. Marçalo is acknowledged for the ESI-MS analyses which were run on a QITMS instrument acquired with the support of the Programa Nacional de Reequipamento Científico (Contract REDE/1503/REM/2005 — ITN) of Fundação para a Ciência e a Tecnologia and is part of RNEM — Rede Nacional de Espectrometria de Massa.

Appendix A. Supplementary data

Supplementary data to this article can be found online at doi:10.1016/j.jinorgbio.2011.01.013.

References

[1] M. Gielen, E.R.T. Tiekink (Eds.), Metallotherapeutic Drugs and Metal-based Diagnostic Agents: The Use of Metals in Medicine, Wiley, 2005.
[2] S. Roy, P.U. Maheswari, M. Lutz, A.L. Spek, H.D. Dulk, S. Barends, G.V. Wezel, F. Hartl, J. Reedijk, Dalton Trans. (2009) 10846–10860.
[3] S. Zhang, C. Tu, X. Wang, Z. Yang, J. Zhang, L. Lin, J. Ding, Z. Guo, Eur. J. Inorg. Chem. (2004) 4028–4035.
[4] R.S. Kumar, K. Sasikala, S. Arunachalam, J. Inorg. Biochem. 102 (2008) 234–241.
[5] L.D. Pachon, A. Golobic, B. Kozlevcar, P. Gamez, H. Kooijman, A.L. Spek, J. Reedijk, Inorg. Chim. Acta 357 (2004) 3697.
[6] P.U. Maheswari, S. Roy, H. den Dulk, S. Barends, G. van Wezel, B. Kozlevcar, P. Gamez, J. Reedijk, J. Am. Chem. Soc. 128 (2006) 710–711.

[7] P.U. Maheswari, S. Barends, S. Özalp-Yaman, P. Hoog, H. Casellas, S.J. Teat, C. Massera, M. Lutz, A.L. Spek, G.P. van Wezel, P. Gamez, J. Reedijk, Chem. Eur. J. 13 (2007) 5213–5222.
[8] F. Silva, F. Marques, I.C. Santos, A. Paulo, A.S. Rodrigues, J. Rueff, I. Santos, J. Inorg. Biochem. 104 (2010) 523–532.
[9] M. Videira, F. Silva, A. Paulo, I.C. Santos, I. Santos, Inorg. Chim. Acta 362 (2009) 2807–2813.
[10] D.D. Perrin, W.L.F. Armarego (Eds.), Purification of LaboratoryChemicals, Oxford, 1988.
[11] W. SADABS, Area-Detector Absorption Correction, Brukee AXS Inc., Madison, WI, 2004.
[12] M. SAINT, Area-Detector Integration Software. (Version 7.23), Brukee AXS Inc., Madison, WI, 2004.
[13] A. Altomare, M.C. Burla, M. Camalli, G.L. Cascarano, C. Giacovazzo, A. Guagliardi, A. Grazia, G. Moliterni, G. Polidori, R. Spagna, J. Appl. Crystallogr. 32 (1999) 115–119.
[14] G.M. Sheldrick, SHELXL-97: Program for the Refinement of Crystal Structure, University of Gottingen, Germany, 1997.
[15] L.J. Farrugia, J. Appl. Crystallogr. 32 (1999) 837–838.
[16] L.J. Farrugia, J. Appl. Crystallogr. 30 (1997) 565.
[17] J.R. Aranzaes, M.C. Daniel, D. Astruc, Can. J. Chem. Rev. Can. Chim. 84 (2006) 288–299.
[18] N. Butenko, A.I. Tomaz, O. Nouri, E. Escribano, V. Moreno, S. Gama, V. Ribeiro, J.P. Telo, J.C. Pesssoa, I. Cavaco, J. Inorg. Biochem. 103 (2009) 622–632.
[19] A.W. Addison, T.N. Rao, J. Reedijk, J. van Rijn, G.C. Veschoor, J. Chem. Soc. Dalton Trans. (1984) 1349–1356.
[20] S.-L. Ma, X.-X. Sun, S. Gao, C.-M. Qi, H.-B. Huang, W.-X. Zhu, Eur. J. Inorg. Chem. (2007) 846–851.
[21] W.E. Marsh, K.C. Patel, W.E. Hatfield, D.J. Hodgson, Inorg. Chem. 22 (1983) 511–515.
[22] C.P. Pradeep, P.S. Zacharias, S.K. Das, J. Chem. Sci. 117 (2005) 133–137.
[23] E.D. Estes, W.E. Estes, W.E. Hatfield, D.J. Hodgson, Inorg. Chem. 14 (1975) 106–109.
[24] D.W. Phelps, W.H. Goodman, D.J. Hodgson, Inorg. Chem. 15 (1976) 2266–2270.
[25] D.D. Swank, G.F. Needham, R.D. Willett, Inorg. Chem. 18 (1979) 761–765.
[26] F. Tuna, L. Patron, Y. Journaux, M. Andruh, W. Plass, J.-C. Trombe, J. Chem. Soc. Dalton Trans. (1999) 539–545.
[27] M. Rodriguez, A. Llobet, M. Corbella, A.E. Martell, J. Reibenspies, Inorg. Chem. 38 (1999) 2328–2334.
[28] N.R. Sangeetha, S. Pal, Polyhedron 19 (2000) 1593–1600.
[29] A.M. Schuitema, A.F. Stassen, W.L. Driessen, J. Reedijk, Inorg. Chim. Acta 337 (2002) 48–52.
[30] M. Du, Y.-M. Guo, X.-H. Bu, J. Ribas, M. Monfort, New J. Chem. 26 (2002) 645–650.
[31] W.A. Alves, R.H.d.A. Santos, A. Paduan-Filho, C.C. Becerra, A.C. Borin, A.M.D.C. Ferreira, Inorg. Chim. Acta 357 (2004) 2269–2278.
[32] H. Liu, F. Gao, D. Niu, J. Tian, Inorg. Chim. Acta 362 (2009) 4179–4184.
[33] A.G. Orpen, L. Brammer, F.H. Allen, O. Kennard, D.G. Watson, R. Taylor, Dalton Trans. (1989) S1–S83.
[34] W.A. Alves, S.A.d. Almeida-Filho, R.H.d.A. Santos, A. Paduan-Filho, A.M.d.C. Ferreira, J. Braz. Chem. Soc. 15 (2004) 872–883.
[35] C. Bovet, A. Barron, Electron Paramagnetic Resonance Spectroscopy of Copper(II) Compounds, Digital Scholarship at Rice University, U.S.A, http://cnx.org/content/m22507/1.2/.
[36] A. Rockenbauer, L. Korecz, Appl. Magn. Reson. 10 (1996) 29–43.
[37] U. Sakaguchi, A.W. Addison, Dalton Trans. (1979) 600–608.
[38] M. Valko, R. Klement, P. Pelikan, R. Boca, L. Dlhan, A. Boettcher, H. Elias, L. Mueller, J. Phys. Chem. 99 (1995) 137–143.
[39] I. Correia, A. Dornyei, T. Jakusch, F. Avecilla, T. Kiss, J.C. Pessoa, Eur. J. Inorg. Chem. (2006) 2819–2830.
[40] R. Shakya, F. Peng, J. Liu, M.J. Heeg, C.N. Verani, Inorg. Chem. 45 (2006) 6263–6268.
[41] D. Chen, M. Frezza, R. Shakya, Q.C. Cui, V. Milacic, C.N. Verani, Q.P. Dou, Cancer Res. 67 (2007) 9258–9265.
[42] S.S. Hindo, M. Frezza, D. Tomco, M.J. Heeg, L. Hryhorczuk, B.R. McGarvey, Q.P. Dou, C.N. Verani, Eur. J. Med. Chem. 44 (2009) 4353–4361.